Electronic Supplementary Material (ESI) for RSC Advances.

Calcium Vapor Synthesis Of Extremely Coercive $SmCo_5$

Sarah E. Baker[1], Alexander A. Baker[1*], Chris A. Orme[1], Matthew Worthington[1], Tian Li[1], Edwin M. Sedillo[1], Jessica Dudoff [1], Jonathan R. I. Lee[1], Joshua D. Kuntz[1], Scott K. McCall[1]*

[1] Lawrence Livermore National Laboratory, Livermore, CA 94550, USA.

Initial magnetization

Examining the initial magnetization of a sample from the virgin state can reveal additional information about magnetization reversal mechanisms, as discussed in the main text. **Figure S1** shows the initial magnetization of a molded sample reduced for 12 hours. The sharp increase in magnetization at low fields points to domain wall motion being the primary driver of reversal in this range.

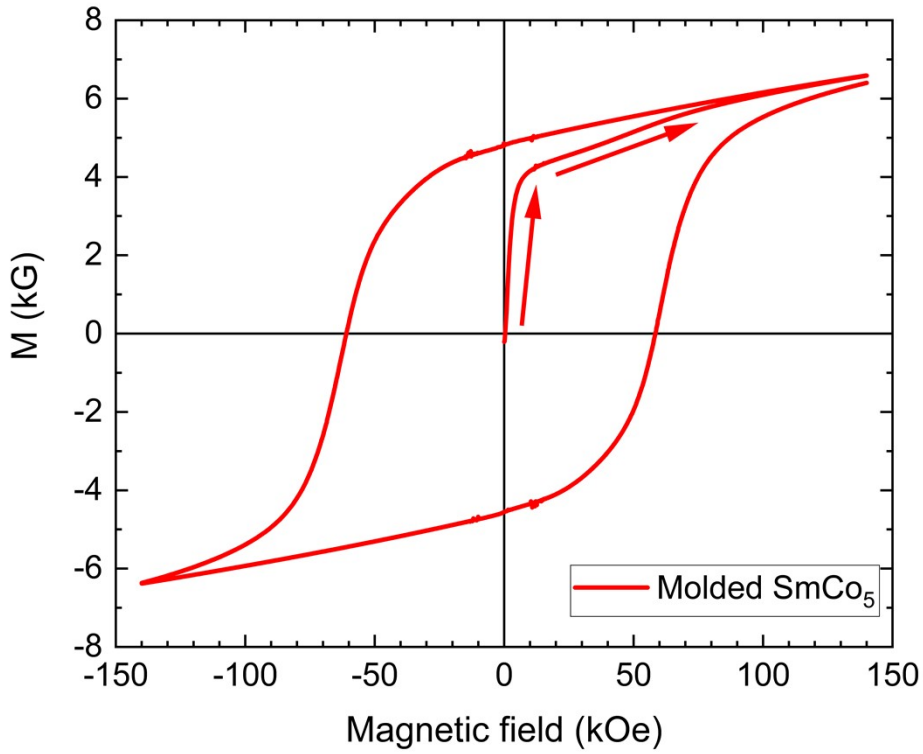

Figure S1: Initial magnetization of a molded sample reduced under forming gas and Ca vapor for 12 hours. Note the sharp increase in the initial magnetization at low fields, followed by gradual reorientation above 1T, which points to pinning-type magnetization reversal rather than coherent rotation of domains.

Micromagnetic Model

A micromagnetic model of magnetization reversal assumes the measured coercivity, $H_{c,i}$, is determined by the nucleation field, H_n, and then reduced by effective demagnetization, N_{eff}, and the parameter α_{eff}, which incorporates the effects of misaligned grains, inhomogeneities in material parameters, and thus pinning strength. Note that as an effective demagnetizing parameter, N_{eff} can locally exceed 1 in regions where flux lines are concentrated and is dimensionless. Such regions can function as nucleation sites for reverse domain nucleation during the switching process. H_n is therefore the coercivity expected for a defect free, ellipsoidal, uniaxial particle with easy axis parallel to the applied field, and is reduced by the factors contained within N_{eff} and α_{eff} as[1]:

$$H_{c,i} = \alpha_{eff} H_n - N_{eff} M_s \quad (1)$$

Where M_s is the saturation magnetization of the ferromagnet. Following Singh et al[1], we note that the nucleation field in $SmCo_5$ is determined primarily by the anisotropy constant, and use the substitution $H_n = 2K_1/4\pi M_s$. This analysis is complicated by the fact that the samples were so coercive that they could not be fully saturated in the available 14 kOe field, but it provides a useful framework to consider the temperature evolution of magnetic properties. Using values of the anisotropy constant taken from studies on single crystals,[2] the relationship between the normalized coercivity and normalized nucleation field can be determined, and is plotted for EPD and molded samples in Fig. S2. Taking a linear fit to the region $2K_1/JM_s^2 < 100$ and extracting the gradient and intercept yields the following values:

Molded: $N_{eff} = 2.7 \pm 0.5$; $\alpha_{eff} = 0.133 \pm 0.007$

EPD: $N_{eff} = 1.5 \pm 0.4$; $\alpha_{eff} = 0.152 \pm 0.006$

The high demagnetization factors indicate the presence of strongly concentrated magnetic flux lines, leading to large local stray fields.[1] The values of $\alpha_{eff} < 0.35$ point to a reversal mechanism that is a mix of both nucleation of domains from areas of locally enhanced demagnetization, and the pinning at grain boundaries or other defects. [1,3] The deviation from purely linear behaviour likely arises from the limits of using the maximum measured magnetization in place of the true saturation magnetization.

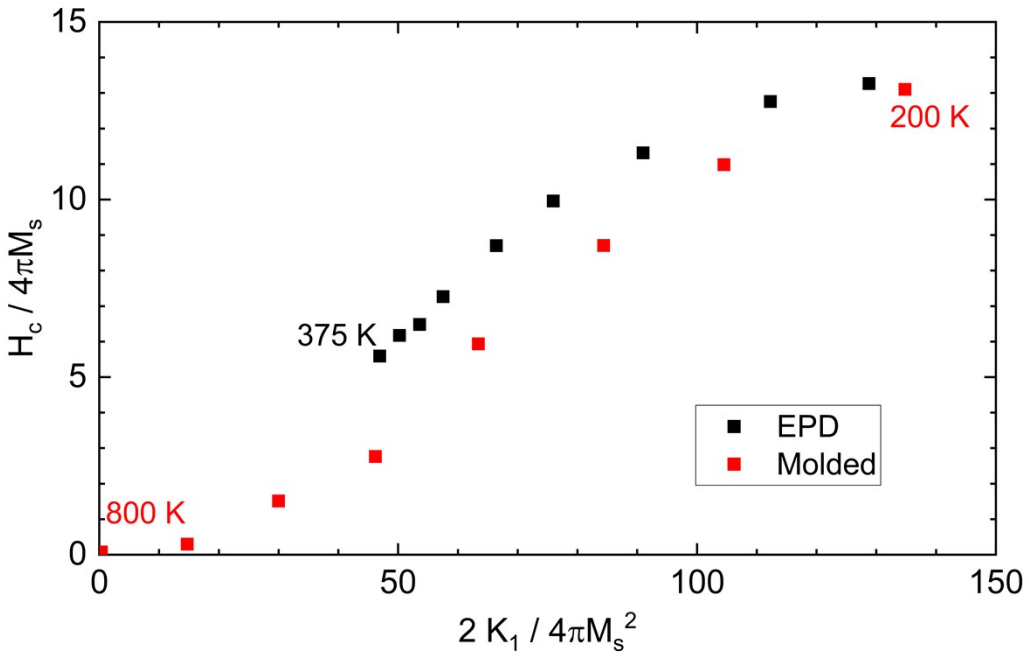

Figure S2: Micromagnetic analysis of molded and EPD samples using a parametric plot of temperature dependence fit to equation 1 (see text).

Alternative Reduction Strategies

KCl has been reported as an effective high temperature solvent for Sm-Co-O nanoparticles,[4] leading to coercivities of ~20 kOe. Trials conducted on flame sprayed nanopowders, however, found KCl to be inimical to the formation of magnetically hard particles, with a typical result shown in **Figure S3**. Similarly, direct mixing of the oxide nanoparticles with Ca metal led to low coercivities.

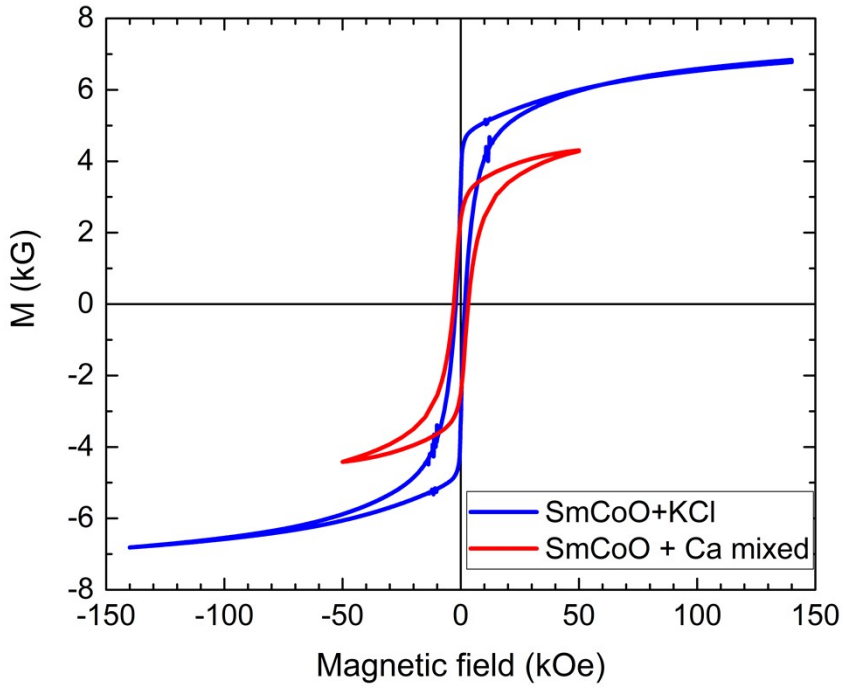

Figure S3: M(H) for a sample reduced in the presence of KCl, or with Ca mixed with the powder resulting in coercivities 10 kOe at ambient temperature.

Sources of Data for Figure 2b

Figure 2b and **Figure S4** compare the magnetization and coercivity of calciothermically reduced samples with reports from literature and industry. Here the sources of the example data are shown. Arnold Magnetics is representative of high-quality industrially available materials, while other suppliers offer similar performing SmCo products. Note that these samples are often SmCo5/Sm2Co17 mixes, with additional Zr, Fe, Cu, and other additives to enhance the properties.

Anisotropic magnets are also included in this plot, demonstrating the performance metrics that may be achieved if the grains are aligned to impose a preferred orientation.

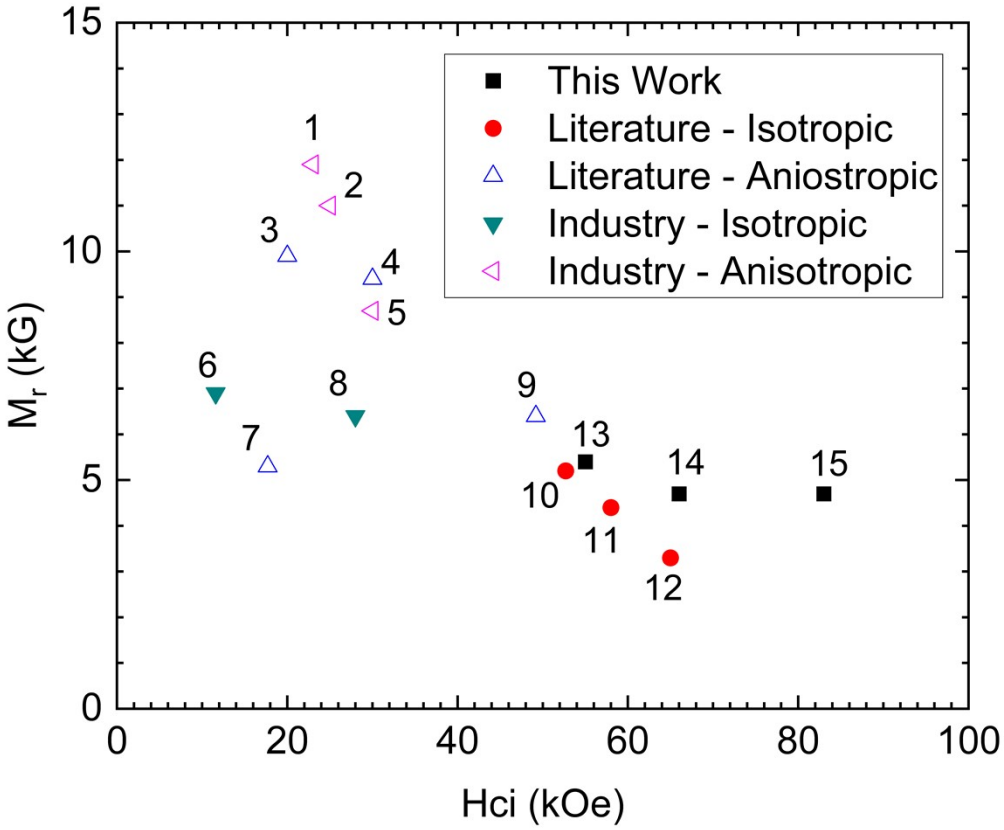

Figure S4: As Fig. 2(b) in main text, labelled, with anisotropic magnets included. The remnant magnetization and coercivity at room temperature are compared with reports from literature, and commercially available SmCo magnets.

Table S1: Data for Fig. S3, collected from literature and online sales brochures. This list is far from exhaustive and is for illustrative purposes only. Note $H_{c,I}$ here refers to the intrinsic coercivity measured from an M(H) hysteresis loop.

NUMBER	SOURCE	$H_{C,I}$	M_R
1	Arnold Magnetics – Recoma 35E	23	11.9
2	Arnold Magnetics – Recoma 28	25	11
3	Reference [5]	20	9.9
4	Reference [1]	30	9.4
5	Arnold Magnetics – Recoma 18	30	8.7
6	Arnold Magnetics 2101 injection molded	11.6	6.9
7	Reference [6]	17.7	5.3
8	Arnold Magnetics	28	6.4
9	Reference [7]	49.2	6.4
10	Reference [8]	52.7	5.2
11	Reference [9]	58	4.4
12	Reference [10]	65	3.3
13	This work - EPD	55	5.4
14	This work – molded	66	4.7

15	This work - dropcast	83	4.7

1 A. Singh, V. Neu, S. Fähler, K. Nenkov, L. Schultz and B. Holzapfel, *Phys. Rev. B*, 2008, **77**, 104443.
2 B. Barbara and M. Uehara, *IEEE Trans. Magn.*, 1976, **12**, 997–999.
3 H. Kronmüller, K.-D. Durst and M. Sagawa, *J. Magn. Magn. Mater.*, 1988, **74**, 291–302.
4 C. Yang, L. Jia, S. Wang, C. Gao, D. Shi, Y. Hou and S. Gao, *Sci. Rep.*, 2013, **3**, 3542.
5 W. Szmaja, J. Grobelny and M. Cichomski, *Appl. Phys. Lett.*, 2004, **85**, 2878–2880.
6 B. Z. Cui, A. M. Gabay, W. F. Li, M. Marinescu, J. F. Liu and G. C. Hadjipanayis, *J. Appl. Phys.*, 2010, **107**, 09A721.
7 B. Shen, C. Yu, A. A. Baker, S. K. McCall, Y. Yu, D. Su, Z. Yin, H. Liu, J. Li and S. Sun, *Angew. Chem. Int. Ed Engl.*, 2019, **58**, 602–606.
8 S. Koppoju, V. Chandrasekaran and R. Gopalan, *AIP Adv.*, 2015, **5**, 077118.
9 J. Ding, P. A. I. Smith, P. G. McCormick and R. Street, *J. Magn. Magn. Mater.*, 1996, **161**, 303–308.
10 Y. Liu, M. P. Dallimore, P. G. McCormick and T. Alonso, *J. Magn. Magn. Mater.*, 1992, **116**, L320–L324.